# Chemical Substitution in $Ba(RE_{1/2}Nb_{1/2})O_3$ (RE = La, Nd, Sm, Gd, Tb, and Y) Microwave Ceramics and Its Influence on the Crystal Structure and Phonon Modes

Anderson Dias,[§] L. Abdul Khalam,[†] Mailadil T. Sebastian,[†] Carlos William A. Paschoal,[⊥] and Roberto L. Moreira*[,‡]

*Departamento de Engenharia Metalúrgica e de Materiais, Universidade Federal de Minas Gerais, Rua Espírito Santo 35, Sala 206, Belo Horizonte-MG 30160-030, Brazil, Ceramic Technology Division, Regional Research Laboratory, Trivandrum 695 019, India, Departamento de Física, Instituto de Ciências Exatas, Universidade Federal de Minas Gerais, C. P. 702, Belo Horizonte-MG 30123-970, Brazil, and Departmento de Física, CCET, Universidade Federal do Maranhão, São Luís, Maranhão 65085-580, Brazil*

*Received September 2, 2005. Revised Manuscript Received November 1, 2005*

Raman spectroscopy was employed to evaluate the crystal structure and phonon modes of chemically substituted $Ba(RE_{1/2}Nb_{1/2})O_3$ microwave ceramics (RE = La, Nd, Sm, Gd, Tb, and Y). It was verified that these materials could be divided into tetragonal (ceramics with RE = Y, Tb, and Gd) and orthorhombic (RE = Sm, Nd, and La) structures. Lorentzian lines were used to fit the spectra, which presented 9 bands for the first group and 23 bands for the second group of ceramics. The position and width of the phonon modes were determined, and were correlated to the ionic radii and tolerance factors for the different atoms substituted in the *B*′-site. It is believed that simple rotational distortions of the oxygen octahedra led to the occurrence of structures other than cubic, which is very difficult to detect by X-ray diffraction or even spectroscopic techniques.

## Introduction

Ceramics with perovskite-related $ABO_3$ structures are well-known technological materials because of their ability to be employed in a wide variety of present-day applications.[1] In this respect, the cellular communication industry has been experiencing a remarkable change since the development of ceramic materials that can be used as dielectric resonators and filters to store and transfer microwave communication signals.[2,3] Particularly, the complex perovskites with nonideal *A*−O and *B*−O bond distances and distorted noncubic symmetries are likely to be part of future developments needed in high-frequency communication and in several other integrated technologies.[4] Nowadays, practically all ceramic systems are studied in an attempt to find applications in this growing market, with complex tantalate ceramics receiving the most attention.[5] The many possibilities of the perovskite structures in the mixed-cation formula $AA'[B'B'']O_3$ are mainly due to the variety of chemistry principles that can be combined (ionic radii, valence, tolerance factor, etc.) to obtain innumerable compounds with a variety of properties, designed for many integrated devices.

For microwave dielectrics, it is possible to specify some minimum requirements, such as that dielectric constants must be constrained between 35 and 55 (defines the size of the resonator), temperature coefficients of the resonance frequency must be chemically tunable close to zero (affects the device frequency stability), and quality factors must be greater than 20 000 (production of low-noise oscillators and narrow-band filters).[3] Filter designers prefer to use complex tantalates derived from $Ba(Zn_{1/3}Ta_{2/3})O_3$ and $Ba(Mg_{1/3}Ta_{2/3})O_3$ because of their higher selectivity and optimizing bandwidth.[6] This high demand for tantalum increased its price, and redirected studies to new compositions based on isostructural niobium compounds. However, problems with the temperature coefficient of the resonant frequency and the quality factors still remain. Among the compositions currently under study, $Ba(Mg_{1/3}Nb_{2/3})O_3$ and $A(RE_{1/2}Nb_{1/2})O_3$ (*A* = Ba and Sr, RE = rare-earth elements) presented interesting properties that can be applied in microwave frequencies.[7−10]

Complex $Ba(RE_{1/2}Nb_{1/2})O_3$ (BRN) ceramics have been studied in the last 10 years by many research groups in an attempt to understand their crystal structure as a function of chemical substitution on the *B*′-site, but conclusive results on this subject are still not possible. The structural and

* To whom correspondence should be addressed. Telephone: 55 31 34995624. Fax: 55 31 34995620. E-mail: bmoreira@fisica.ufmg.br.

§ Departamento de Engenharia Metalúrgica e de Materiais, Universidade Federal de Minas Gerais.

† Regional Research Laboratory.

⊥ Universidade Federal do Maranhão.

‡ Departamento de Física, Instituto de Ciências Exatas, Universidade Federal de Minas Gerais.

(1) Bhalla, A. S.; Guo, R.; Roy, R. *Mater. Res. Innovations* **2000**, *4*, 3.
(2) Wersing, W. *Curr. Opin. Solid State Mater. Sci.* **1996**, *1*, 715.
(3) Cruickshank, D. *J. Eur. Ceram. Soc.* **2003**, *23*, 2721.
(4) Vanderah, T. A. *Science* **2002**, *298*, 1182.
(5) Cava, R. J. *J. Mater. Chem.* **2001**, *11*, 54.
(6) Hughes, H.; Iddles, D. M.; Reaney, I. M. *Appl. Phys. Lett.* **2001**, *79*, 2952.
(7) Moreira, R. L.; Matinaga, F. M.; Dias, A. *Appl. Phys. Lett.* **2001**, *78*, 428.
(8) Dias, A.; Moreira, R. L. *J. Appl. Phys.* **2003**, *94*, 3414.
(9) Moreira, R. L.; Andreeta, M. R. B.; Hernandes, A. C.; Dias, A. *Cryst. Growth Des.* **2005**, *5*, 1457.
(10) Ratheesh, R.; Wöhlecke, M.; Berge, B.; Wahlbrink, T.; Haeuseler, H.; Rühl, E.; Blachnik, R.; Balan, P.; Santha, N.; Sebastian, M. T. *J. Appl. Phys.* **2000**, *88*, 2813.

10.1021/cm051982f CCC: $33.50 
Published on Web 12/09/2005

microwave dielectric properties of these materials were investigated by direct microwave measurements as well as by Raman and Fourier transform infrared spectroscopies.[11−18] In this respect, the polar optical phonons determine the high-frequency dielectric response, which in turn depends on the sample structure (intrinsic contributions) together with extrinsic contributions coming from space charges, domain walls, and imperfections linked to the sample morphology. Although the conflicting dielectric constants appeared to be solved after the work of Khalam et al.,[17] the reported crystal structures are reported to be noncubic or slightly different from cubic. Tetragonal, orthorhombic, and monoclinic symmetries are also possible in BRN ceramics, depending upon the chemistry involved, i.e., the rare-earth ion and the resulting tolerance factor. It has been suggested that the difference in the crystal symmetry is due to the small tilting in the octahedra, anti-phase or in-phase, which causes a splitting in some X-ray diffraction peaks, and the determination of the true crystal structure is difficult.

In view of that, the goal of the present work is to investigate the crystal structure and phonon modes of BRN ceramics by Raman spectroscopy. The vibrational bands of the ceramics with different chemical substitution on the *B*′-site (La, Nd, Sm, Gd, Tb, or Y) were determined, and the results allow us to contribute to the understanding of the crystalline structure of this system on the basis of group theory analysis. Microwave properties and the vast crystal chemistry resources and principles, such as ionic radii and tolerance factors, are also discussed in light of the knowledge produced here.

## Experimental Section

The dielectric ceramics were prepared by the conventional solid-state ceramic route, in which the starting materials were high-purity $BaCO_3$ (Aldrich Chemicals; 99.9%), $Nb_2O_5$ (Nuclear Fuel Complex, Hyderabad; 99.9%), and rare-earth oxides (Indian Rare Earths Ltd.; 99.99%). The materials were mixed and ball milled using distilled water for 36 h. The mixtures were calcined twice in platinum crucibles at 1375 °C for 4 h. The calcined powders were ground and mixed thoroughly with 4 wt % PVA solution, and were dried and uniaxially pressed at 150 MPa in cylindrical compacts of 10−14 mm. The pellets were initially fired at a rate of 6 °C/min up to 800 °C and then at a rate of 12 °C/min to the sintering temperature (1575−1600 °C), for 4 h in air. Ceramics with La, Nd, Sm, and Gd were produced without a sintering aid, and densities greater than 97% were obtained. Materials with Tb and Y presented poor sinterability and 0.5−1 wt % $CeO_2$ was employed as a sintering aid. For these ceramics, final densities of 98 and 96% were obtained, respectively.

X-ray diffraction (XRD) experiments were carried out in a Rigaku Dmax 1C instrument using Cu Kα radiation (40 kV, 30 mA) and a graphite-monochromator, from 10 to 140° $2\theta$ at a speed of 0.02° $2\theta$/s. Particular $2\theta$ ranges were slowly scanned together with accumulation times of 25 s for each 0.05° $2\theta$. This procedure was necessary where the low resolution made it difficult to determine the definition of peaks for confirming probable splits that could indicate a lower-symmetry structure. The lattice parameters were determined as the average of the calculated values from the prominent reflections of powder diffraction. The errors in the lattice parameters were calculated using the root sum of squares (RSS) method.[19] The indexing of the peaks was performed by using the cards of the International Committee for Diffraction Data (ICDD).

Infrared reflectance spectra were recorded in a Fourier transform spectrometer (Bomem DA 8-02) equipped with a fixed-angle specular reflectance accessory (external incidence angle of 11.5°). In the mid-infrared region (500−4000 $cm^{-1}$), we used a SiC globar lamp as the infrared source, and also used a Ge-coated KBr beam splitter and a $LN_2$-cooled HgCdTe detector. In the far-infrared range (50−600 $cm^{-1}$), we employed a mercury-arc lamp, a 6 $\mu$m coated Mylar hypersplitter, and a LHe-cooled Si-bolometer. One of the ceramic faces received a thin gold coating, and was used as a rough mirror for the reference spectra. This procedure allowed us to improve the reflectivity spectra, as the mirror surface mimics the sample one, which compensates for the effects of the diffuse reflection at the sample surface. The measurements were performed at a pressure of $10^{-4}$ bar and a resolution of 2 $cm^{-1}$. The reflectivity spectra were evaluated by means of standard Kramers−Kronig analysis, and were adjusted by an oscillator model. A generalized four-parameter oscillator model[20] was used rather than the classical model to achieve a good fit with a minimum number of physically meaningful oscillators. Unfortunately, we were not able to discern from the results the bands expected for lower-symmetry structures. Our spectra showed a maximum of 6 bands, and no improvements could be added to the work of Zurmühlen et al.[13]

Micro-Raman scattering spectra were collected at room temperature using a triple-monochromator Dilor XY spectrometer, equipped with a liquid-$N_2$-cooled charge-coupled device (CCD) detector and an Olympus microscope (100× objective). All slits and optics of the spectrometers were set to give a spectral resolution better than 2 $cm^{-1}$. The measurements were carried out in backscattering geometry using the 415.6, 488, or 632.8 nm lines of argon−krypton and helium−neon ion lasers as excitation sources. All measurements were performed using a long-working-distance plane−achromatic objective (50×/80×/100×). The accumulation times were typically 10 collections of 20 s, and the collected spectra were fitted by a sum of Lorentzian lines. Better results were obtained for the helium−neon laser line than for the argon−krypton line.

## Results and Discussion

Although the crystalline structures obtained through XRD analysis of BRN materials are interpreted as being cubic ($Fm\bar{3}m$) in most of the works, numerous reasons lead the authors to observe that the actual structures "deviate slightly from cubic". This verification is repetitively stressed, and a definitive solution to this problem is always postponed. In the present work, the elements Y, Tb, Gd, Sm, Nd, and La were chosen for use in determining the crystalline structures

(11) Gregora, I.; Petzelt, J.; Pokorny, J.; Vorlocek, V.; Zikmund, Z.; Zurmühlen, R.; Setter, N. *Solid State Commun.* **1995**, *94*, 899.
(12) Koshy, J.; Kurian, J.; Thomas, J. K.; Yadava, Y. P.; Damodaran, A. D. *Jpn. J. Appl. Phys.* **1994**, *33*, 117.
(13) Zurmühlen, R.; Petzelt, J.; Kamba, S.; Voitsekhovskii, V.; Colla, E.; Setter, N. *J. Appl. Phys.* **1995**, *77*, 5341.
(14) Sreemoolanadhan, H.; Ratheesh, R.; Sebastian, M. T.; Mohanan, P. *Mater. Lett.* **1997**, *33*, 161.
(15) Kurian, J.; Pai, S. P.; James, J.; Koshy, J. *J. Mater. Sci.* **2001**, *12*, 173.
(16) Ikawa, H.; Takemoto, M. *Mater. Chem. Phys.* **2003**, *79*, 222.
(17) Khalam, L. A.; Sreemoolanathan, H.; Ratheesh, R.; Mohanan, P.; Sebastian, M. T. *Mater. Sci. Eng. B* **2003**, *107*, 264.
(18) Levin, I.; Prosandeev, S. A.; Maslar, J. E. *Appl. Phys. Lett.* **2005**, *86*, 011919.
(19) Surendran, K. P.; Sebastian, M. T.; Mohanan, P.; Moreira, R. L.; Dias, A. *Chem. Mater.* **2005**, *17*, 142.
(20) Gervais, F. In *Infrared and Millimeter Waves*; Button, K. J., Ed.; Academic Press: New York, 1983; Vol. 8.

**Table 1. Structural Parameters for the Microwave Ceramics Investigated**

| ceramics | RE ionic radius (Å) | tolerance factor | ICDD card | structure |
|---|---|---|---|---|
| $Ba(Y_{1/2}Nb_{1/2})O_3$ | 0.900 | 0.98597 | 24-1042 | cubic |
| $Ba(Tb_{1/2}Nb_{1/2})O_3$ | 0.923 | 0.98067 | 37-0858 | tetragonal |
| $Ba(Gd_{1/2}Nb_{1/2})O_3$ | 0.938 | 0.97725 | 34-0976 | tetragonal |
| | | | 47-0378 | cubic |
| $Ba(Sm_{1/2}Nb_{1/2})O_3$ | 0.958 | 0.97272 | 37-0857 | orthorhombic |
| | | | 47-0377 | cubic |
| $Ba(Nd_{1/2}Nb_{1/2})O_3$ | 0.983 | 0.96712 | 14-0116 | cubic |
| | | | 47-0376 | cubic |
| $Ba(La_{1/2}Nb_{1/2})O_3$ | 1.032 | 0.95633 | 37-0856 | monoclinic |

as a function of the chemical substitution in BRN ceramics. Table 1 presents the materials studied together with the ionic radii, tolerance factors, and the ICDD cards available for indexing. A gradual increase in the ionic radii corresponds to a decrease in the tolerance factors, determined by

$$t = \frac{R_A + R_O}{\sqrt{2}\left[\left(\frac{R_{B'} + R_{B''}}{2}\right) + R_O\right]} \quad (1)$$

where $R_A$, $R_{B'}$, $R_{B''}$, and $R_O$ are the radii of the *A*, *B*′, *B*″, and O ions, respectively. All structures present tolerance factors less than unity, which means that the $NbO_6$ and $REO_6$ octahedra are tilted, because the Ba ions (located in the *A*-site) have too much space for vibrations resulting in large anharmonicity.

We have conducted XRD experiments, and the results lead us to conclude that our samples belong to two distinct crystalline structures. The first type includes Y, Tb, and Gd, whereas Sm, Nd, and La can be grouped in a second type. Preliminary XRD analysis showed that the first group has identical spectra, except for the shift presented by the variation in the ionic radii, and could be indexed according to the available ICDD cards as cubic $Fm\bar{3}m$ (Y and Gd) and tetragonal $I4/m$ (Tb). However, a more careful analysis revealed a split in the peak at around 70° 2$\theta$ for all ceramics (Figure 1), which is not expected for cubic samples. According to the ICDD cards analyzed, only Tb-containing

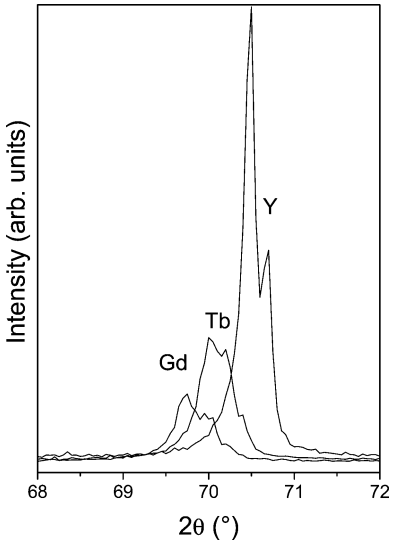


**Figure 1.** XRD for the microwave ceramics with Y, Tb, and Gd. Detail for the range 68−72° 2$\theta$, in which the peak splitting indicates a tetragonal structure.

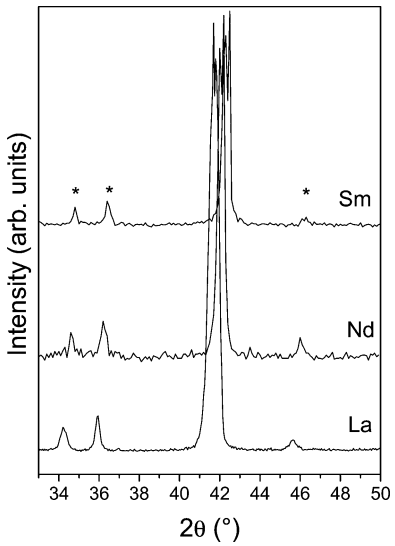


**Figure 2.** Difractograms for the materials with Sm, Nd, and La. Detail for the range 33−50° 2$\theta$, in which asterisks denote peaks compatible only with an orthorhombic structure.

materials (ICDD 37-0858) would present this split because of their tetragonal structure. Also, as pointed out by Koshi et al. (ICDD card 47-378),[12,21] the ceramic with gadolinium can exhibit lower symmetry depending on the heat treatment employed. For Y-containing compounds, Zurmühlen et al.[22] found a satisfactory fit of the neutron diffraction data with the tetragonal space group $I4/m$ for the ceramic with tantalum, suggesting the antiphase tilting of the $TaO_6$ octahedra as the origin of the structural distortion. Gregora et al.[11] extended these results for niobium compounds with Y and Gd, and confirmed a cubic-to-tetragonal transition with temperature. Thus, we conclude that the possibility of this tetragonal structure must be seriously considered for this first group of materials.

For the second type of microwave ceramics, similar XRD analysis was observed together with the expected shift in the peaks as a function of the ionic radii. The ICDD cards available index them as cubic, except for Sm, which presents the possibility for an orthorhombic structure (ICDD 37-0857). Figure 2 shows the diffractograms for this group of materials in a particular 2$\theta$ region. After a rigorous analysis, we believe that an orthorhombic structure could be assumed, especially considering the split in the peak at around 42° 2$\theta$ (orthorhombic) and the absence of the peak at 48° 2$\theta$ (present in the cubic structure) for the ceramic with samarium. Also, the diffractogram of the neodymium could not be well-indexed by cubic ICDD cards. For the lanthanum samples, the presence of the peaks at around 34, 36, and 46° 2$\theta$ excludes the possibility of indexing this ceramic as monoclinic. Thus, on the basis of the XRD analyses, this second group of microwave materials appeared to be better-described by an orthorhombic structure.

The difficulties in identifying small structural distortions in cubic lattices lead us to employ Raman spectroscopy, a very sensitive technique for probing order−disorder and for

(21) Koshy, J.; Thomas, J. K.; Kurian, J.; Yadava, Y. P.; Damodaran, A. D. *Mater. Lett*. **1993**, *17*, 393.
(22) Zurmühlen, R.; Colla, E.; Dube, D. C.; Petzelt, J.; Reaney, I. M.; Bell, A.; Setter, N. *J. Appl. Phys*. **1994**, *76*, 5864.

determining structures of symmetry lower than cubic. The ideal $ABO_3$ cubic perovskite presents no Raman-active modes ($Pm\bar{3}m$), whereas perovskites with a loss of translational symmetries or that are less symmetric have Raman lines.[23] For complex cubic perovskites of general formula $A(B'_{1/2}B''_{1/2})O_3$, $Fm\bar{3}m$ symmetry is expected in ordered lattice arrangements with a 1:1 ratio. This configuration allows for a classification of the normal modes at the Brillouin zone-center as

$$\Gamma = A_g \oplus E_g \oplus F_{1g} \oplus 2F_{2g} \oplus 5F_{1u} \oplus F_{2u} \qquad (2)$$

The resulting factor-group analysis indicates that 4 modes are Raman-active ($A_g$, $E_g$, $F_{2g}$), and also that 4 modes are infrared-active ($F_{1u}$).[23] For our samples, XRD data show that an $Fm\bar{3}m$ structure is not possible, which agrees with the literature available so far. The previous results help us start the group theory analysis on a more realistic basis. Assuming the conclusions from our XRD data are correct, BRN ceramics could be described as belonging to the $C_{4h}^5(I4/m)$ group ($Z = 2$), for Y, Tb, and Gd, and to the $D_{2h}^{16}(Pbnm)$ group, for Sm, Nd, and La ($Z = 2$). For the first structure (tetragonal), the Ba atoms occupy 4*d* sites of special $S_4$ symmetry, the *B*′ and Nb ions occupy 2*a* and 2*b* sites of $C_{4h}$ symmetry, and the oxygen atoms are in the 8*h* and 4*e* sites ($C_s$ and $C_4$ symmetries, respectively). It is then possible, using the site-group method of Rousseau et al.,[24] to obtain the following distribution of irreducible representations of the $C_{4h}$ point group

$$\Gamma = 3A_g \oplus 5A_u \oplus 3B_g \oplus B_u \oplus 3E_g \oplus 6E_u \qquad (3)$$

Excluding the acoustic modes ($A_u \oplus E_u$), we would expect 9 Raman modes ($A_g$, $B_g$, $E_g$) and 9 infrared bands ($A_u$, $B_u$) for this group. Let us then assume the centrosymmetric *Pbnm* space group (orthorhombic) for the second type of microwave ceramics. In this case, rare-earth and niobium ions should occupy the 4*b* Wyckoff-site of $C_i$ symmetry, Ba and O(1) ions occupy 4*c* sites of $C_s^{xz}$ symmetry, and O(2) and O(3) occupy 8*d* sites of general $C_1$ symmetry. The site-group method now leads to the following distribution of irreducible representations of the $D_{2h}$ point group

$$\Gamma = 7A_g \oplus 8A_u \oplus 5B_{1g} \oplus 10B_{1u} \oplus 7B_{2g} \oplus 8B_{2u} \oplus 5B_{3g} \oplus 10B_{3u} \qquad (4)$$

For Sm, Nd, and La materials, we would expect 24 Raman modes ($7A_g \oplus 5B_{1g} \oplus 7B_{2g} \oplus 5B_{3g}$) and 25 independent infrared ones ($9B_{1u} \oplus 7B_{2u} \oplus 9B_{3u}$). These phonons correspond to vibrations of $Ba^{2+}$ cations ($2A_g \oplus A_u \oplus B_{1g} \oplus 2B_{1u} \oplus 2B_{2g} \oplus B_{2u} \oplus B_{3g} \oplus 2B_{3u}$), oxygen atoms ($5A_g \oplus 4A_u \oplus 4B_{1g} \oplus 5B_{1u} \oplus 5B_{2g} \oplus 4B_{2u} \oplus 4B_{3g} \oplus 5B_{3u}$), and vibrational motions of RE/Nb atoms ($3A_u \oplus 3B_{1u} \oplus 3B_{2u} \oplus 3B_{3u}$).

Figure 3 presents the Raman spectra of all microwave ceramics studied in the present work. The intensities are in log scale to reveal details in the weaker lines as well as the strongest ones. In general, the samples have a highly ordered structure because the Raman peaks are of narrow line width. Another immediate conclusion is that the ceramics, definitively, are not cubic, as the $O_h^5(Fm\bar{3}m)$ symmetry for a 1:1 order would present only 4 bands. It is also clear that two types of Raman spectra are observed: the first one with little more than 7 bands (Y, Tb, and Gd ceramics), and the second one with at least 18 phonon modes (Sm, Nd, and La materials). The exact number of bands is determined only after detailed analysis performed by fitting with Lorentzian lines. The weak features at 169, 213, and 435 $cm^{-1}$ in the Y spectrum were not considered in our analyses because they appear only for this particular compound, and seem to be associated with some defective modes rather than with intrinsic Raman modes of the crystal lattice. The measured spectra show that the vibrational behavior of our Ba($RE_{1/2}Nb_{1/2}$)$O_3$ perovskites is very similar to that of other complex perovskites of general formula $A(B'_{1/2}B''_{1/2})O_3$, $A(B'_{1/3}B''_{2/3})O$, and $A(B'_{2/3}B''_{1/3})O_3$, which allow us to assign the observed bands in the same way as that proposed previously.[7,23,25] The two groups of microwave ceramics will be treated separately in the following paragraphs.

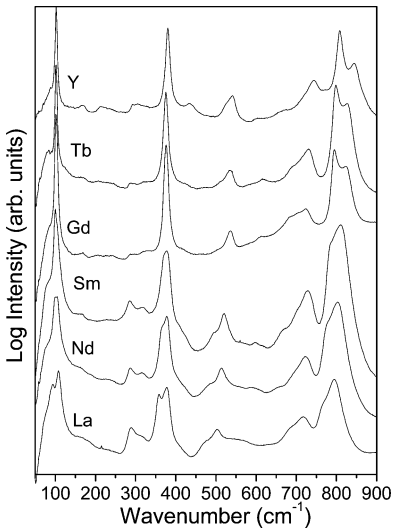


**Figure 3.** Raman spectra for all samples studied. Intensity is in the log scale.

**Table 2. Raman Fitting Parameters for the Microwave Ceramics with Y, Tb, and Gd**

| | Ba($Y_{1/2}Nb_{1/2}$)$O_3$ | | Ba($Tb_{1/2}Nb_{1/2}$)$O_3$ | | Ba($Gd_{1/2}Nb_{1/2}$)$O_3$ | |
|---|---|---|---|---|---|---|
| band | frequency ($cm^{-1}$) | fwhm ($cm^{-1}$) | frequency ($cm^{-1}$) | fwhm ($cm^{-1}$) | frequency ($cm^{-1}$) | fwhm ($cm^{-1}$) |
| 1 | 102.3 | 3.2 | 102.0 | 4.6 | 102.2 | 6.7 |
| 2 | 305.4 | 56.7 | 302.9 | 60.5 | 297.5 | 69.3 |
| 3 | 380.1 | 6.8 | 375.4 | 9.7 | 376.0 | 9.7 |
| 4 | 434.3 | 35.9 | 435.3 | 33.0 | 431.3 | 27.8 |
| 5 | 537.4 | 23.3 | 533.3 | 53.4 | 535.1 | 21.2 |
| 6 | 715.6 | 30.2 | 688.8 | 57.3 | 681.8 | 37.5 |
| 7 | 743.1 | 26.0 | 729.5 | 33.4 | 718.9 | 34.6 |
| 8 | 808.5 | 12.4 | 799.3 | 14.6 | 795.6 | 14.9 |
| 9 | 842.7 | 27.2 | 826.7 | 32.4 | 822.9 | 45.3 |

For the group with Y, Tb, and Gd, Figure 3 also shows that the Raman bands are practically the same, except for the modes at frequencies higher than 650 $cm^{-1}$. Table 2 presents the Raman frequency and full width at half-

(23) Siny, I. G.; Tao, R.; Katiyar, R. S.; Guo, R.; Bhalla, A. S. *J. Phys. Chem. Solids* **1998**, *59*, 181.
(24) Rousseau, D. L.; Bauman, R. P.; Porto, S. P. S. *J. Raman Spectrosc.* **1981**, *10*, 253.
(25) Maczka, M.; Hanuza, J.; Fuentes, A. F.; Morioka, Y. *J. Phys.: Condens. Matter* **2004**, *16*, 2297.

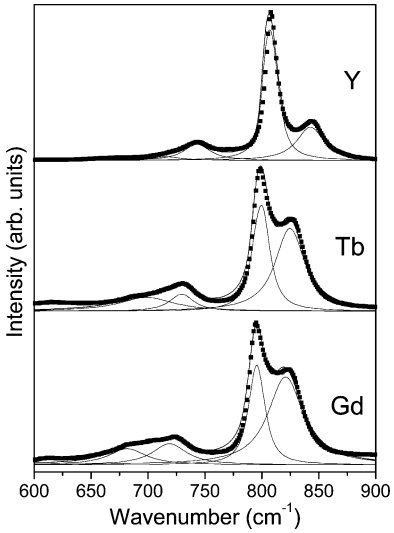


**Figure 4.** Raman spectra for the ceramics with Y, Tb, and Gd. Lorentzian lines (4 curves) fit the experimental data in the region 600−900 $cm^{-1}$.

maximum (fwhm) parameters for the materials with Y, Tb, and Gd. As can be seen, 9 bands were found after fitting, as previously mentioned, and practically no variation was observed in frequency for bands below 600 $cm^{-1}$, which are related to Ba ($A_{1g} \oplus E_g$) and Ba−O ($A_{1g}$) vibrations (translational motions) and are insensitive to chemical substitution on *B*-sites. The region between 100 and 300 $cm^{-1}$ is normally affected by composition ($A_{1g} \oplus E_g$), but no change was observed because of invariance in the cation on the *B*″-site (Nb) in the studied samples. For frequencies above 600 $cm^{-1}$, a shift to lower frequencies (red shift) was detected as a function of the rare-earth ions from Y to Gd. Figure 4 shows the resulting fit of the 600−900 $cm^{-1}$ region for the microwave ceramics, which better illustrate this behavior. This frequency range represents the vibrations of the oxygen octahedra with RE/Nb cations on their interior. Changes in the composition will affect the modes, especially the $A_{1g}$(O) peaks at 843−823 $cm^{-1}$ (totally symmetric stretching of the $NbO_6$ octahedra). Besides the shift to lower frequencies as the ionic radii increase (or as the tolerance factors decrease), it is important to note the increase in the intensity of the bands at 715−680 and 843−823 $cm^{-1}$. These results also corroborate our assumption for tetragonal structure $C_{4h}^5(I4/m)$ for the ceramics containing Y, Tb, and Gd.

Ratheesh et al.[10] classified their strontium-based ceramics in two categories, and observed a spectral change in the $F_{2g}$ mode near 415 $cm^{-1}$ (shoulder) and a more or less symmetric $A_{1g}$ mode at around 800 $cm^{-1}$ for Y, Tb, and Gd. Ba-based analogues studied here showed different behavior, particularly in the case of the last mode, which presented stronger bands at 843−823 $cm^{-1}$ as the ionic radii increased from Y to Gd. Unlike our conclusions for the Sr-based compounds, we cannot consider our Ba-based ceramics with Y, Tb, and Gd to be cubic. The fwhm for the $A_{1g}$(O) phonon (Table 2) increased from Y to Gd (27−45 $cm^{-1}$), indicating that the $NbO_6$ octahedral cage suffered a weakening with the chemical substitution in the neighboring octahedra. Thus, less tightly bonded cages led to lower quality factors. In fact, Khalam et al.[17] observed a marked decrease in the quality factors for these tetragonal ceramics, from 49 600 (Y) to 5700 (Gd).[17] Also, Maczka et al.[25] observed a clear correlation between the ionic radii of lanthanides and yttrium cations and the wavenumbers of the $A_{1g}$ mode, which decreased with increasing ionic radii of the cation in the order Gd, Tb, Y (Tables 1 and 2). This can be attributed to the decrease in the *B*′−O bond length, and was predicted by lattice dynamic calculations.[25]

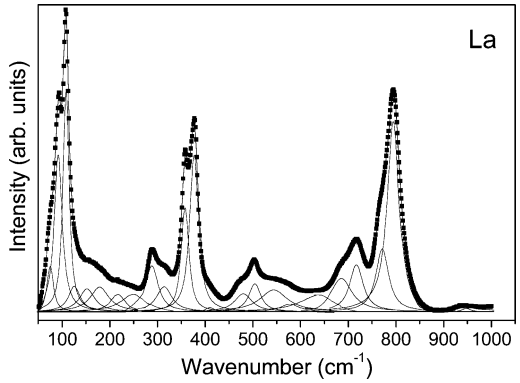


**Figure 5.** Raman spectrum for the La-containing microwave ceramic. The experimental data were fitted with a sum of 23 Lorentzian curves.

Let us now analyze the Raman spectra of the second group of materials. For these ceramics, we have proposed orthorhombic symmetry $D_{2h}^{16}(Pbnm)$, with 24 expected Raman modes. Lorentzian lines were employed to fit the experimental data (Sm, Nd, and La), which showed similar behavior for all materials. The final result is presented in Figure 5 for the ceramic $Ba(La_{1/2}Nb_{1/2})O_3$. As can be seen, a good fit was obtained, and a total of 23 bands could be adjusted to the experimental curve. Ratheesh et al.[10] analyzed the Raman spectra of rare-earth strontium niobates, and showed a reduction in symmetry for the $Sr(B'_{1/2}Nb_{1/2})O_3$ complex perovskites when trivalent ions with larger ionic radii were located at the *B*′-site. For ceramics with Sm, Nd, and La, the authors have verified completely different spectra from those observed for Y, Tb, and Gd. Shoulders in the $A_{1g}$ mode were correlated to a possible tilting or distortion of the octahedra. For these materials, we agree with the assumptions of Ratheesh et al. that a tetragonal structure seems to be inappropriate and that a lower-symmetry structure is probably the correct one for Sm, Nd, and La compounds. Table 3 shows the Raman frequencies and fwhm for the ceramics with Sm, Nd, and La studied here. As a general trend, the frequencies decreased and the fwhm increased with increasing RE ionic radii. When comparing the second group of materials with the first group, we observed similar behavior for the bands related to Ba motions, which practically presented an invariant tendency. The higher number of modes in this group made the assignment of all bands difficult, but confirms without doubt the orthorhombic structure. Khalam et al.[17] measured the microwave dielectric properties of $Ba(RE_{1/2}Nb_{1/2})O_3$ for samples containing Sm, Nd, and La, and observed a substantial decrease in the quality factors, from 18 400 (Sm) to 5700 (La). This decrease can be correlated to the Raman parameter fwhm for the $A_{1g}$(O) mode (811−796 $cm^{-1}$), which increased as a result of the less tightly bonded $NbO_6$ cages and was influenced by the chemical substitution in the neighboring octahedra. The decrease in the *B*′−O bond

**Table 3. Raman Fitting Parameters for the Microwave Ceramics with Sm, Nd, and La**

| | $Ba(Sm_{1/2}Nb_{1/2})O_3$ | | $Ba(Nd_{1/2}Nb_{1/2})O_3$ | | $Ba(La_{1/2}Nb_{1/2})O_3$ | |
|---|---|---|---|---|---|---|
| band | frequency ($cm^{-1}$) | fwhm ($cm^{-1}$) | frequency ($cm^{-1}$) | fwhm ($cm^{-1}$) | frequency ($cm^{-1}$) | fwhm ($cm^{-1}$) |
| 1 | 81.6 | 12.6 | 79.5 | 10.9 | 75.2 | 14.5 |
| 2 | 99.8 | 6.7 | 98.8 | 10.4 | 91.9 | 18.9 |
| 3 | 105.6 | 8.8 | 105.7 | 9.9 | 108.4 | 13.6 |
| 4 | 121.0 | 19.1 | 118.4 | 25.7 | 125.6 | 29.0 |
| 5 | 147.4 | 29.6 | 142.1 | 34.5 | 152.3 | 38.3 |
| 6 | 178.8 | 43.5 | 173.4 | 40.0 | 178.6 | 46.3 |
| 7 | 221.7 | 39.9 | 223.7 | 33.3 | 214.9 | 35.2 |
| 8 | 252.3 | 42.7 | 253.6 | 35.2 | 249.4 | 40.7 |
| 9 | 284.9 | 33.0 | 286.2 | 33.8 | 288.3 | 29.2 |
| 10 | 318.3 | 47.9 | 317.8 | 42.3 | 314.1 | 36.9 |
| 11 | 364.0 | 21.0 | 368.4 | 20.7 | 357.9 | 15.8 |
| 12 | 376.4 | 11.6 | 379.2 | 11.0 | 376.9 | 19.1 |
| 13 | 405.0 | 28.9 | 413.2 | 28.8 | 409.9 | 27.4 |
| 14 | 493.7 | 37.3 | 481.6 | 37.0 | 480.0 | 41.4 |
| 15 | 519.2 | 21.1 | 513.7 | 24.6 | 503.9 | 27.4 |
| 16 | 549.3 | 44.7 | 540.6 | 47.6 | 543.5 | 67.7 |
| 17 | 605.3 | 36.9 | 588.3 | 40.5 | 577.4 | 45.1 |
| 18 | 661.9 | 55.5 | 634.0 | 70.0 | 636.8 | 90.5 |
| 19 | 704.6 | 30.8 | 689.2 | 42.4 | 685.6 | 51.8 |
| 20 | 728.5 | 22.4 | 722.6 | 30.3 | 717.1 | 32.1 |
| 21 | 788.7 | 21.3 | 780.7 | 24.4 | 771.3 | 33.3 |
| 22 | 811.0 | 29.1 | 803.8 | 35.5 | 795.6 | 38.3 |
| 23 | 995.3 | 27.1 | 976.9 | 28.5 | 947.6 | 28.9 |

length (from La to Sm) can also contribute to the red shift of the $A_{1g}$ mode, as verified by Maczka et al.[25]

Now, the question is why it is so difficult to establish the correct structure for these materials, or why the cubic structure was assumed for such a long time with all the contradictory results and evidence that indicated a structure that was at least "slightly deviated from cubic". It is probably because these materials present structural distortions of the ferroelastic type that arise from octahedral rotations and/or displacements of atoms. Recently, X-ray absorption fine structure (XAFS) spectroscopy was applied to obtain direct quantitative information about the local structure of mixed-ion perovskites.[26,27] Shuvaeva et al.[26] used XAFS to probe the local structure of lead-free relaxor ferroelectrics, and observed that although the technique is not sufficient to construct a whole structural model, it provides values of displacements of transition metal atoms in complex ceramics. The authors observed that changes in the macroscopic symmetry did not affect the local environment of atoms, and that the local structure could be highly distorted even in cubic phases. In another work, Shuvaeva et al.[27] studied the local environment of Nb atoms in Pb-containing perovskite compounds, and verified that Nb occupies an off-center position with a symmetry lower than that observed by macroscopic symmetry. This result introduced a new concept regarding phase transitions and order−disorder behavior, as local distortions quantified by advanced spectroscopic techniques appeared to be much larger than the average distortions observed using X-ray diffraction.

In the present work, we believe that the distortions in BRN ceramics occur with small or large tilts of the octahedral cages in order to optimize the $A$−O bonds by lowering the coordination number around the *A*-site cation. For very small tilts, the XRD technique is not appropriate, and the reported data frequently do not observe splits or features, indicating a higher-symmetry structure. However, the tolerance factor is well-known, and is intensively used to understand structural transitions or large tilts of the octahedra.[1,13,22,28] Flerov et al.[29] studied phase transitions in elpasolites, which are ordered perovskites with the general formula $A_2B'B''X_6$ (in ref 29, $X$ is a halogen atom). The authors defined the stability range of the cubic structure on the basis of the tolerance factor (or the degree of tilt) for many compounds with many combinations of cations. Their results showed that the decrease in the tolerance factor with increasing ionic radii is followed by a change of the cubic symmetry to tetragonal symmetry at room temperature, depending on the combination of atoms. When ions approach the border of the stability range (defined by the tolerance factor), bond stresses between halogen ions and their neighbors can produce small tilts that change the structure.[29] According to this approach, the stability of the cubic phase is governed by the ratio between the size of the individual atoms and the lattice parameter. For elpasolites, Flerov et al. verified that the sum of the ionic radii of atoms lying on the edge of the cubic cell is larger than that of the lattice parameter. The conclusion is that the instantaneous position of the halogen atoms in the $B'-X-B''-X-B'$ and $A-X$ chains is not on the edge. The increase in bond stress is equivalent to an increase in the repulsive energy contribution to the potential energy of crystal, and leads to an increase in the vibrational anisotropy of the $X$ atoms and a simultaneous decrease in the initial phase stability.[29] Thus, changes in the sizes of atoms can modify the temperature of the phase transitions, and can even inhibit the occurrence of a structural distortion.

In our samples, oxygen is the atom that suffers the stresses generated by the chemical substitution on the $B'$-site, and similar to the elpasolites, our samples show a lowering of symmetry as a function of the atom present in the material. The crystallographic and group theoretical analysis of the structural phase transitions in perovskite and perovskite-like crystals is reviewed by Alexandrov et al.[30] These authors verified that the initial structures are distorted by one kind of tilt or by superposition of tilts in the slabs. Most of the tilts correspond to symmetry changes, which can be associated with definite vibrational lattice modes of the initial structure. For the first group of materials studied in the present work, we believe that a structural distortion occurred from the initial cubic $O_h^5(Fm\bar{3}m)$ phase through the tilt of the oxygen octahedra. Figure 6 illustrates this simple rotational distortion of the perovskite structure toward the tetragonal $C_{4h}^5(I4/m)$ symmetry, as also verified by Flerov et al.[29] and Alexandrov et al.[30] Rotations of the type cubic → tetragonal can be understood as a tilt of the type (000) → (00$\phi$) that occurs in adjacent layers in opposite directions (dotted octahedra rotate toward the full octahedra in Figure

(26) Shuvaeva, V. A.; Zekria, D.; Glazer, A. M.; Jiang, Q.; Weber, S. M.; Bhattacharya, P.; Thomas, P. A. *Phys. Rev. B* **2005**, *71*, 174114.
(27) Shuvaeva, V. A.; Pirog, I.; Azuma, Y.; Yagi, K.; Sakaue, K.; Terauchi, H.; Raevskii, I. P.; Zhuchkov, K.; Antipin, M. Y. *J. Phys.: Condens. Matter* **2003**, *15*, 2413.
(28) Reaney, I. M.; Colla, E. L.; Setter, N. *Jpn. J. Appl. Phys.* **1994**, *33*, 3984.
(29) Flerov, I. N.; Gorev, M. V.; Aleksandrov, K. S.; Tressaud, A.; Grannec, J.; Couzi, M. *Mater. Sci. Eng., R* **1998**, *24*, 81.
(30) Alexandrov, K. S.; Bartolome, J. *Phase Transitions* **2001**, *74*, 255.

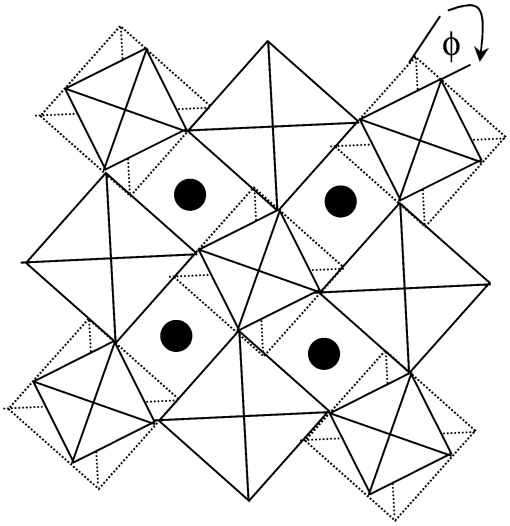


**Figure 6.** Simple rotational distortion of the perovskite structure as a result of octahedral tilts. The structural transition from the initial cubic $O_h^5(Fm\bar{3}m)$ to tetragonal $C_{4h}^5(I4/m)$ symmetry occurs by rotation of the dotted octahedra of adjacent layers in opposite directions. The new lattice parameters are $a = b = 0.707a_0$, $c = a_0$ ($a_0$ is the original cubic lattice parameter). Full circles represent Ba atoms.

6). With regard to the initial lattice parameter $a_0$, the new parameters are now $a = b = 0.707a_0$, and $c = a_0$. For the second group of ceramics, complicated distortions of the initial phase are expected, and they probably occur through the superposition of octahedral tilts.

## Conclusions

We have studied the chemical substitution in $Ba(RE_{1/2}Nb_{1/2})O_3$ (RE = La, Nd, Sm, Gd, Tb, and Y) ceramics and its influence on the crystal structure and phonon modes. The results showed that these materials could be grouped in two different structures: tetragonal for Y-, Tb-, and Gd-containing compounds, and orthorhombic for Sm-, Nd-, and La-based materials. Raman spectroscopy was employed to obtain the exact crystal structure and phonon modes. The tetragonal ceramics exhibit 9 active bands, whereas the orthorhombic ones presented 23 vibrational modes when fitted by a sum of Lorentzian curves. The results of Raman analyses were correlated to the microwave dielectric properties, and allow us to conclude that the $A_{1g}$ mode is directly related to these properties when no order−disorder phenomena occur, i.e., broader bands correspond to lower quality factors in $B'$-site-substituted ceramics. The ferroelastic distortions in these materials are connected with simple rotational changes in the octahedral cages, thus modifying the crystal structure (lowering of symmetry) as the RE ionic radii increased (the tolerance factor decreased).

**Acknowledgment.** The Brazilian authors acknowledge financial support from CNPq/MCT (Profix) and FAPEMA. The Indian authors thank Council of Scientific and Industrial Research (CSIR), New Delhi, India. Special thanks to Prof. M. A. Pimenta for his hospitality during Raman experiments.

**Supporting Information Available:** Experimental far-infrared spectra for all samples, fitting curves, and tables with fitting parameters. Notice that IR modes are very broad, which hindered the observation of splitting of the phonon modes. Also, microwave dielectric properties are supplied for the ceramics studied. This material is available free of charge via the Internet at http://pubs.acs.org.

CM051982F